*Proceedings of the 20th International Conference on Soil Mechanics and Geotechnical Engineering– Rahman and Jaksa (Eds)*


# Design and construction challenges of soil nail wall in unsaturated clay with sand lenses

## Les défis de la conception et de la construction d'un mur en sol cloué dans de l'argile non saturée avec des lentilles de sable

**Bosco Poon**
*GHD Pty Ltd, NSW, Australia, bosco.poon@ghd.com*

Peter Mitchell
*The University of Adelaide, SA, Australia*

ABSTRACT: The effective stress concept for unsaturated soils was applied to the design and construction of an 8.9m high soil nail wall excavation as part of an expressway construction in Adelaide, South Australia. As the excavation depth is permanently above the water table, the long-term behaviour of the unsaturated stiff clays involves a component of the shear strength governed by soil suction. Notable design challenges, in the context of unsaturated soil condition, were the development of soil suction profile and the use of appropriate unsaturated soil strength. During construction, the excavation through some of the thick and clean sand lenses within the clay caused significant over-break, leading to greater wall movements than anticipated. Back-analysis using FEA indicated that the unravelling of the exposed sandy soil had resulted in the formation of tension cracks that would lead to a lower FoS than the long-term design requirement. Remedial design with extra soil nails were subsequently installed. This paper describes the geotechnical design of the soil nail wall with the consideration of soil suction, which had to be modified during construction because of sand lenses being encountered. Comparison between the design and measured wall movements is also presented

RÉSUMÉ : Le concept de contrainte effective de sol non saturé a été appliqué à la conception et à la construction d'une excavation de 8,9 m de haut pour un mur en sol cloué dans le cadre de la construction d'une autoroute à Adélaïde, en Australie du Sud. Comme la profondeur de l'excavation est en permanence au-dessus de la nappe phréatique, le comportement à long terme des argiles rigides non saturées implique une composante de la résistance au cisaillement régie par l'aspiration du sol. Dans le cas d'un sol non saturé, les défis de conception notables ont été le développement du profil de succion du sol et l'utilisation d'une résistance appropriée du sol non saturé. Pendant la construction, l'excavation, à travers certaines des lentilles de sable épaisses et propres de l'argile, a provoqué une fissure excessive et significative qui a engendré des mouvements de mur plus importants que prévus. L'analyse rétrospective par éléments finis (AEF) a indiqué que l'effritement du sol sablonneux et exposé avait entraîné la formation de fissures de tension, ce qui conduirait à un CS inférieur aux exigences de conception à long terme. Une conception corrective avec des clous de sol supplémentaires a ensuite été mise en place. Cet article décrit la conception géotechnique du mur en sol cloué, en tenant compte de l'aspiration du sol, qui a dû être modifiée pendant la construction en raison de la présence de lentilles de sable. Une comparaison entre la conception et les mouvements mesurés du mur est également présentée.

KEYWORDS: unsaturated soil strength, soil nail wall, soil suction profile, observational method, design and construction

## 1 INTRODUCTION

The project was a 3.7 km long road upgrade between Torrens Road and the River Torrens located at about 5km northwest of Adelaide CBD. The road upgrade involved the construction of a 3km long lowered road section of up to 8.9m deep cutting with soil nail reinforcement. The project area has a deep Quaternary alluvial profile. The regional groundwater occurs in a gravelly aquifer at depths of about 9 to14m beneath ground surface, which is reflective of the level in the River Torrens. The soil above the aquifer, where the lowered road is formed, is typically stiff to very stiff clays with sandy lenses. The clays are of low to medium plasticity. The soil profile beneath the aquifer is a deep deposition of predominately very stiff to hard clays. As the excavation depth is permanently above the water table, the adopted design philosophy for the soil nail walls considered the unsaturated soil strength governed by the long-term soil suction effect. The geotechnical investigations indicated that no significant soil defects (e.g. fissuring) were present in the clays. It was assumed that if such features exist, they were localised and of limited lateral extent.

## 2 SOIL SUCTION PROFILES

Every soil has a total suction, which is a measure of the potential for the soil to undergo a change in moisture content. The total suction is considered as being the sum of two components, the matric suction and osmotic/solute suction. The definitions for the two components have been described in unsaturated soil mechanics textbooks (e.g. Briaud 2013). The measurement of soil suction is in units of kPa, or alternatively in logarithm of pore water potential, pF. The conversion from kPa to pF is given by:

$$suction\ (kPa) = 9.81 \times 10^{(pF-2)} \quad (1)$$

The Department of Planning, Transport, and Infrastructure (DPTI) of the South Australia (SA) government investigated the soil suction profiles of the project site through a soil wetting process in a piled wall trial located at Robert Street next to the project corridor (see Figure 2a). The in-situ total soil suction values were assessed from psychrometer tests on borehole samples obtained prior to the trial. The clays were in a relatively dry condition and the measured total suctions were up to about pF = 4.8 as shown in Figure 1.

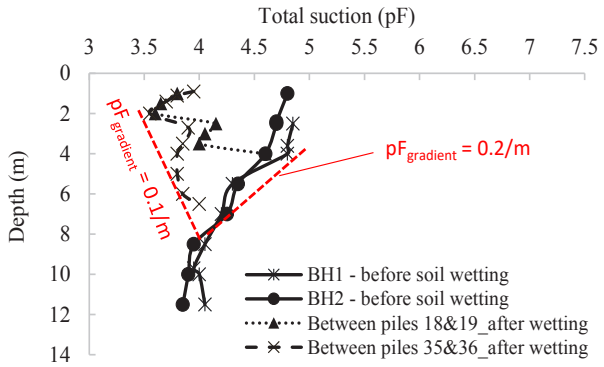


Figure 1. Total suction profiles

After the piled wall excavation to a depth of 8m, water was injected into a 1.5m deep soakage trench located at 1m away from the rear of the wall over a period of 3 to 4 weeks (see Figure 2b). The measured suction values after the soil wetting, as shown in Figure 1, was as low as about pF = 3.6.

For design purposes, pF =3.6 was deemed representative for long-term wetted soil condition and pF = 3.4 was adopted for the adverse case of a prolonged leakage from a broken water pipe.


Figure 2. (a) Trial pit of up to 8m depth, (b) Trench for application of water at the trial

## 3 UNSATURATED SOIL STRENGTH

The shear strength of unsaturated clay was assessed from the equation of Fredlund and Rahardjo (1993):

$$\tau_f = c' + \sigma_v' tan\phi' + u_w tan\phi^b \qquad (2)$$

where $\tau_f$ = shear strength, $c'$ = effective cohesion, $\phi'$= effective friction angle, $\sigma'_v$ = effective stress on failure plane, $u_w$ = matric suction and $\phi^b$ = rate of increase in shear strength with increase in matric suction. For practical design purposes, total suction (i.e. matric suction plus osmotic suction), rather than the matric suction, was used in Eq. 2. This is because the osmotic pressure was much less than the measured total suction, and the total and matric suction curves were almost congruent.

For the fully saturated condition, the effective strength parameters ($c'$ and $\phi'$) were assessed based on 33 CU triaxial test results. A linear regression line drawn through the data points on the p - q plot indicated that $c'$ = 9.5kPa and $\phi'$= 30.7. For design purposes, $c'$ = 5kPa and $\phi'$= 30 were adopted.

To assess the appropriate value of $\phi^b$ under unsaturated condition, test data of Keswick clay in Adelaide by Richards (1977) and Woodburn (1997) was compiled and plotted in Figure 3, which indicates a linear relationship between shear strength and total suction. The mean value of the measured tan $\phi^b$ is 0.15, and the upper and lower bound values were 0.22 and 0.11, respectively. For design purposes, the mean tan $\phi^b$ value of 0.15 was adopted and the corresponding $\phi^b$ value was 8.5°.

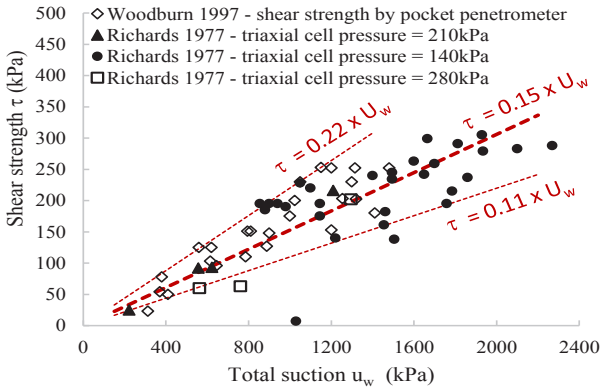


Figure 3. Shear strength vs. total suction

Figure 4 shows a plot of apparent cohesion vs. total suction. In particular, the apparent cohesion of Fredlund and Rahardjo (1993) was obtained from the following specific terms of Eq.2:

$$Apparent\ cohesion = c' + u_w\ tan\phi^b \qquad (3)$$

Eq.3 can be rewritten in term of pF by substituting $c'$ = 5kPa, tan $\phi^b$ = 0.15 and $u_w = 9.81\times10^{(pF\ -\ 2)}$. The assessed apparent cohesion values based on Eq. 3 are much lower than the UU triaxial test results of the unsaturated borehole tube samples that were tested under different cell pressures ranging from 40 kPa to 200 kPa. Conversely, pocket penetrometer (PP) tests on the unsaturated soil samples were not subject to overburden pressures and the results are closer to the prediction by Fredlund and Rahardjo (1993). Note that some soil samples exhibited higher silt and fine sand content, the bonds between the grains were weak and easily broken upon PP testing, leading to lower inferred shear strengths than predictions. Also shown on Figure 4 is the apparent cohesion estimated using Briaud (2013) in conjunction with the effective stress parameter $\chi$ given by Khalili and Khabbaz (1998):

$$Apparent\ cohesion = c' + \chi \cdot u_w\ tan\phi',$$

$$and \qquad \chi \cdot u_w = \sqrt{u_{ae} \cdot u_w} \qquad (4)$$

where $u_{ae}$ is the suction at air entry, which may be taken as 100kPa for Adelaide clays in general. Desa and Scott (2018) presented the project specific soil water characteristic curve (SWCC) of the tested clay samples obtained from the piled wall trial site. The measured air entry value was found to be approximately 275kPa.

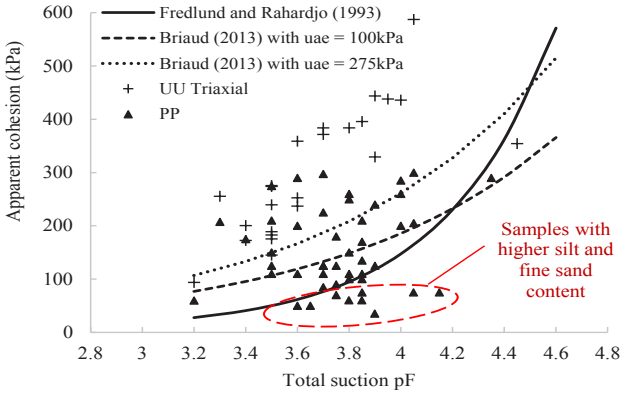


Figure 4. Apparent cohesion vs total suction

By considering both $u_{ae}$ values of 100kPa and 275kPa, Figure 4 shows that the Briaud relationship gives a higher predicted apparent cohesion than that of Eq. 3 at a suction range below pF = 4.2. For design purposes, an apparent cohesion of 40kPa was adopted for long-term design calculated based on

Fredlund and Rahardjo (1993) (i.e. Eq.3) for a design total suction of pF=3.4. This is deemed to be erring on the safe side as the assessed value is generally lower than those of UU triaxial and PP results, as well as that given by Briaud (2013), i.e., Eq. 4.

The stability of the soil nail walls has adopted strength parameters and minimum permissible design Factors of Safety (FoS) appropriate for the various load cases and soil conditions. This method is considered preferable to the use of partial factors (as suggested by AS4678) in unsaturated soils as the analyses are considered to be more transparent. The FoS against global failure presented in Table 1 have been adopted for the wall designs. These FoS are generally consistent with the intent outlined in CIRIA C760 in which moderately conservative, worst credible and most probable scenarios are considered.

Table 1. FoS adopted in design

| Wall Condition | Assumed Soil & Load Conditions | FoS (minimum) |
|---|---|---|
| Temporary – wedge failure mode (1) | Equilibrium soil suction (pF=4.0) | 1.25 |
| Temporary – global stability (2) | Equilibrium soil suction (pF=4.0) | 1.3 |
| Permanent – global stability (2) | Equilibrium soil suction (pF=4.0) | 1.5 |
| Permanent (3) – global stability | Long term wetted soil suction (pF=3.4) | 1.35 |
| Temporary– global (1) | Wetted + earthquake | 1.05 |
| Temporary– global (1) | Wetted + collision | 1.05 |

(1) Worst credible; (2) Most probable; (3) Moderately conservative

## 4 BOND STRESS

DPTI conducted a soil nail trial to inform the design and ultimate soil nail bond strength prior to construction. Two trial sites located at Robert Street and Gawler Street were selected next to the project corridor. The Robert Street site was the previous pile wall trial where soil nails were subsequently installed between the existing piles. At the Gawler Street site the soil nails were installed in the 1V:1H side slopes of a 4m deep excavation. The soils at both sites consisted of very stiff to hard clay/silty clay, with local softening due to controlled soil wetting. A total of 20 pull-out tests were conducted at the trial sites of up to 6m below ground surface. The soil nails used in the trial and later during the production were 25mm threaded steel bars with approved spacers for the support as they were installed with various grouted lengths in 150 or 200mm diameter boreholes that were drilled with rotary drill bit with air flush. Figure 5a shows the frequency histogram of the measured ultimate bond strength during the trial. The mean bond strength value is about 60kPa, which is about 0.3-0.4 times the undrained shear strength $S_u$ of the clay that was estimated to be in the order of 150 – 200kPa. For design purposes, a lower bond strength of 40kPa representing an acceptable 10% failure rate was adopted. This design value was used in stability assessment for short-term cases. For long-term design where the soil was assumed in wetted condition, a geotechnical strength reduction factor of 0.67 was applied, giving a long-term bond stress of 26.7kPa. This is consistent with the lowest pull-out test result of 30kPa in very wet soil condition.

Figure 5b shows the frequency histogram of the measured bond strengths in the acceptance tests during construction. These results are similar to those of the trial, with a mean bond strength value of about 55kPa. However, 10% of the test result were found to be below the design bond strength of 40kPa. The contributory factors for these 10% of soil nails not achieving the design load could be: (i) wetter than expected soil conditions, resulting in loss of soil suction; and (ii) potential remoulding of the soil along the bond zone or inadequately roughened borehole.

Higher ultimate bond strengths were expected for sandy soils, although these soils do not appear to have been tested in the soil nail pull-out trial. The design bond strength for the medium dense and dense sand and silty sand was adopted conservatively as being equal to $\sigma'_{vo} \times \tan 35^\circ$, where $\sigma'_{vo}$ is the effective vertical overburden pressure. However, the collapse of soil nail boreholes in clean sand may lead to a lower bond strength. To overcome this construction difficulty, self-drilling nails were later used for wall excavation in sandy soils. In general, the self-drilling nails achieved a higher pull-out resistance than that of the standard installation method. This was demonstrated by the verification test results. Figure 6 shows an exposed self-drilling nail.

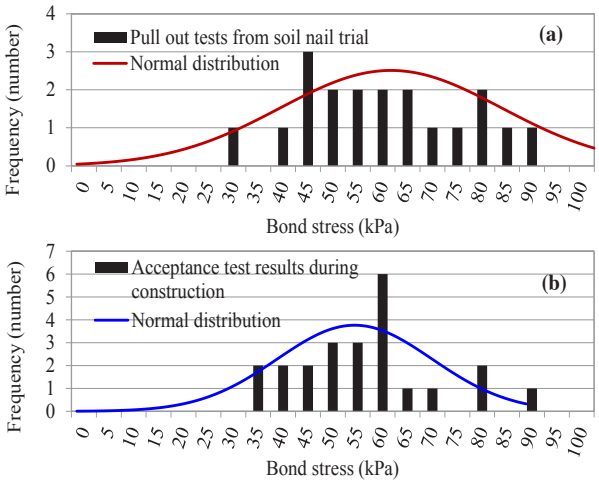


Figure 5. Pull out tests from (a) soil nail trial by DPTI; (b) construction

Figure 6. Self-drilling nail

## 5 WALL DESIGN

The soil nail walls vary in height up to a maximum of about 8.9m. It was constructed at a 1H:40V slope with a 75mm (typical) thick synthetic fiber reinforced shotcrete facing. The drilled holes for the soil nails are inclined at an angle of 15 degrees to the horizontal and are 150mm in diameter, but increased to 200mm diameter in sandy soil and softened clay areas with remoulding issues of the clay soil along the bond zone. The design of the soil nail wall has taken into consideration the global failure mode as well as a nominally 1m wide local wedge failure surface as shown in Figure 7a. Up to five rows of soil nails are adopted, depending on the wall height, proximity to services, and ground condition encountered.

For an 8 m high wall excavation in unsaturated clay, three rows of 4.5 to 6m long soil nails were required (see Figure 7a). The vertical and horizontal spacing between nails were 2.5m and 3m, respectively. For clay profile with interbedded sand lenses, the nail lengths were increased to 5 – 7m and the nail spacing reduced to 1.5m vertically and 2.1m horizontally. The proximity of sewer trench had a marked impact on the global stability, particularly as the upper nail lengths were limited to before the trench in case unforeseen emergency repairs are required. To achieve a satisfactory FoS for wall stability, a layer of geogrid was installed over the trench at the underside of the pavement

(Figure 7b). This is to provide extra tensile reinforcement and alter the failure surface geometry.

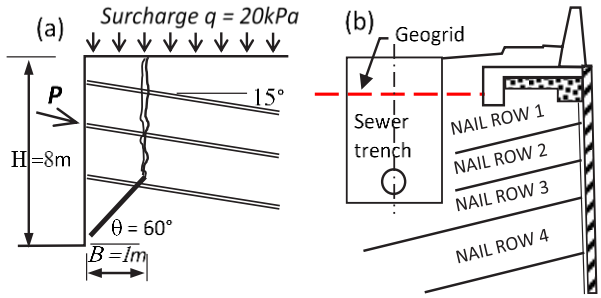


Figure 7. (a) Wedge failure mechanism (b) Design of soil nail wall near existing sewer trench

## 6 OBSERVATIONAL METHOD

An observational method (Figure 8) was adopted for soil nail wall construction, whereby a temporary bench was created in front of each excavation lift, so a visual assessment of the ground conditions could be made. This allowed time for the geotechnical site representative to confirm the ground conditions and to select suitable soil nail arrangements from the toolbox designs that were pre-developed during the detailed design stage for a range of possible soil profiles and unfavorable ground conditions (such as sand lenses, unsaturated fissured clay and perched groundwater). Upon final trim of the temporary bench for each excavation lift, the ground conditions were re-inspected prior to installation of soil nail and shotcrete.

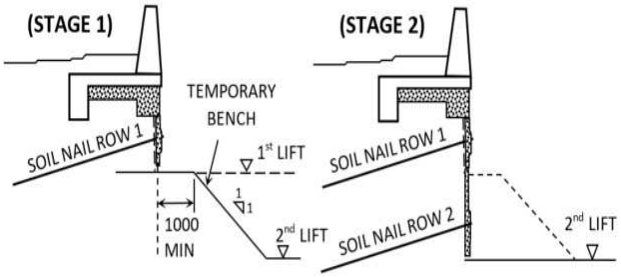


Figure 8. Observational method for soil nail wall construction

## 7 WALL MOVEMENTS DURING CONSTRUCTION

### 7.1 *Wall movements in clay*

Monitoring of soil nail wall excavations was carried out during construction and over the service life using a system of inclinometers and survey markers. For wall excavation in clayey soil profile (typically stiff to very stiff consistency), the measured wall deflection during construction was small. As shown in Figure 9, the maximum deflection was typically less than 0.25% of the excavation depth in clay.

### 7.2 *Wall movements in clay with thick sand lenses*

Sand lenses (pockets of cohesion-less sand and silty sand) of varying thicknesses and of varying depths were encountered in the southern part of the wall alignment. The occurrence of sand lenses at the base or mid-height of a cut was deemed to be more critical to global stability than a sand lens near the top of the wall. Figure 10 shows the sub-soil profile at the southern side of the wall alignment where sand lenses were encountered. The total retaining height at this wall section was 8m and was constructed in staged excavation.

Figure 9. Observed wall deflections in stiff clays

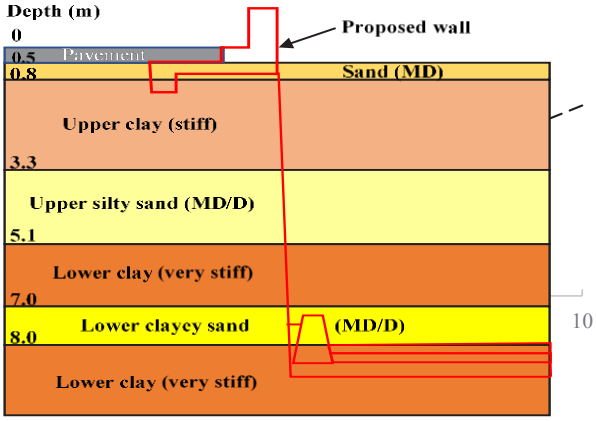


Figure 10. Sub-soil profile at the southern side of the wall alignment

Figure 11. Site photo on the cave-in of the exposed sand layer

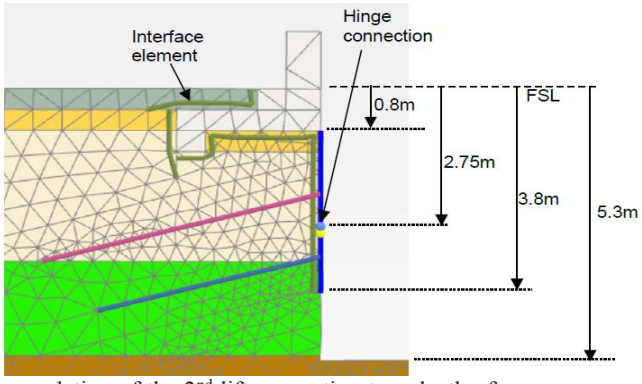


After the completion of the 2nd lift excavation to a depth of 5.3m below wall top, the exposed cut face in silty sand was not covered with shotcrete immediately due to unexpected construction delays. As the exposed face lost moisture, a significant unravelling of the sandy soil occurred that resulted in soil caving-in, with a typical undercut size of 0.5m wide by 1.3m high (Figure 11). Wall movements exceeding design predictions were observed, with a horizontal and vertical displacement of up to 25mm and 14mm, respectively, being measured at the top of wall (Figure 12). Longitudinal cracks of up to 7mm wide were observed at the pavement behind the wall. The cracks were formed parallel with the road alignment at an offset distance of 2 to 2.5m from the inner side of the crash barrier, which coincided with the footing heel of the barrier. Coring investigations along the cracks indicated that they were generally terminated at the bottom of the base course of the pavement structure, of up to about 1m below pavement surface. Notwithstanding the surface cracks outlined, the wall top deflection was at 0.47% of the excavated depth, which remained within 0.2 to 0.5% range commonly observed for wall excavation in stiff clays.

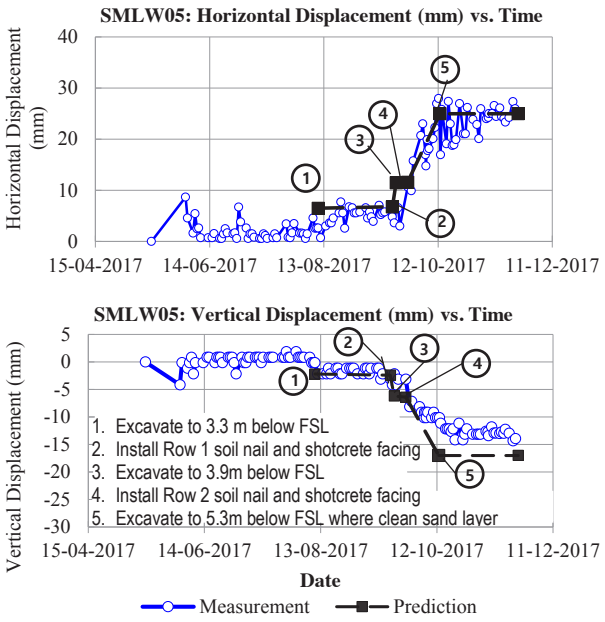


Figure 12. Back-analysed wall movements vs. measurements

In light of the wall movements, back-analysis based on 2D FEA using the PLAXIS 2D was carried out. Figure 13 depicts the configurations of the shotcrete and soil nails adopted in the model for the current state. In essence, the shotcrete has been constructed in two stages. The first stage of shotcrete was installed from depth 0.8 (underside of the barrier footing) to depth 2.75 m below FSL. The second stage was installed at depths 2.75 m to 3.8 m below FSL. Hinge connection was introduced in the FE model to create a joint between the two stages of shotcrete installation, such that the shotcrete ends can rotate freely without transfer of bending moment at the joint.

The back-analysis undertaken was a short-term analysis using undrained shear strengths as inputs for all clayey soils. All soil materials are modelled using Mohr-Coulomb model. This relatively simple model is considered adequate for the present assessment, which is mainly focused on wall movements, as opposed to other excavation induced soil movements such as ground loss at the retained surface or soil heave at the bottom of the excavation. The adopted soil model and engineering properties for back-analysis are summarised in Table 2 with the following points highlighted:

- The adopted short term undrained shear strength ($S_u$) for both the upper and lower clay layers was 125kPa since the material was generally very stiff to hard with PP reading of 250kPa or greater and SPT N ranging from 13 – 26. Note that for the long-term cases, the unsaturated long-term strengths outlined in Section 3 were used.
- the CPT soundings through the clay materials have registered a cone resistance ($q_c$) of generally 5MPa to 10MPa. The use of the conventional method for saturated soil mechanic and neglecting suction influence on CPT result will lead to an overestimation of soil strength for unsaturated condition.
- The adopted undrained Young's modulus $E_u$ for the clays was assessed based on $E_u = 300 \times S_u$, whereas for sands on $E' = 4\ q_C$ was adopted with an average $q_c$ of 10MPa.
- The adopted coefficient of earth pressure at rest, $K_0$, for the clayey soils in the undrained analysis is 1.0, which is consistent with the expected value encountered in Adelaide city (Kaggwa, 1992). For sandy soils, the adopted $K_0$ is 0.5.

Figure 13. FE model for back-analysis

Table 2. Adopted parameters for back-analysis (short term analysis)

| Material | $S_u$ (kPa) | c′ (kPa) | ϕ′ (°) | E (MPa) | Bond stress (kPa) |
|---|---|---|---|---|---|
| Upper clay | 125 | – | – | 37.5 | 35 |
| Upper sand | – | 0 | 35 | 40 | 35 |
| Lower clay | 125 | – | – | 37.5 | 40 |
| Lower sand | – | 0 | 34 | 35 | 40 |

The back-analysis results matched successfully with the measured top of wall displacement as shown in Figure 12. The volumetric strain plot (Figure 14) obtained from FEA exhibits similar features to those of observed including: (i) a potential wedge failure at the exposed cut face; and (ii) a shallow crack zone behind the footing heel of the crush barrier.

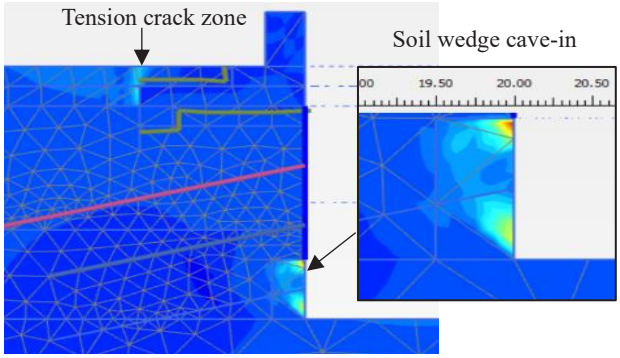


Figure 14. Volumetric strain plot from FEA showing potential tension crack and cave-in

The global stability of current state of the wall was assessed in the FE analysis using a c'- ϕ'reduction approach from PLAXIS, and supplemented by a conventional limit equilibrium using Morgenstern Price method of slices from SLOPE/W. The assessed Factor of Safety (FoS) using FEA approach is presented in Figure 15. It can be seen that the assessed shape of the failure surface and the corresponding FoS value from the FEA are commensurate with those given by the traditional limit equilibrium method shown in Figure 16. Further, both analyses indicate a FoS for the wall that was considered acceptable for short-term construction.

While the assessed FoS is satisfactory for short term excavation to mid-height of the wall, the formation of tension cracks has resulted in a lower assessed FoS than 1.35 after full depth excavation under the adverse long-term wetted soil suction condition (pF=3.4). Extra soil nails were installed as part of the remedial design to accommodate the formation of the 1m wide tension crack zone extending to 2m depth behind the footing heel of the crush barrier. Figure 17 shows the remedial design configurations with extra soil nails and Figure 18 shows the finished wall after full depth excavation.

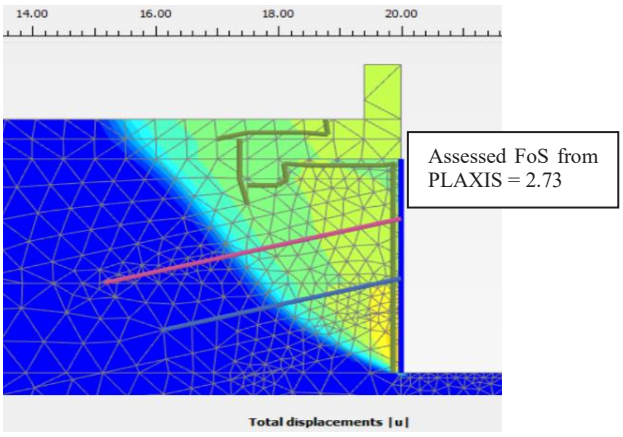

Figure 15. Assessed critical failure surface and FoS using FEA

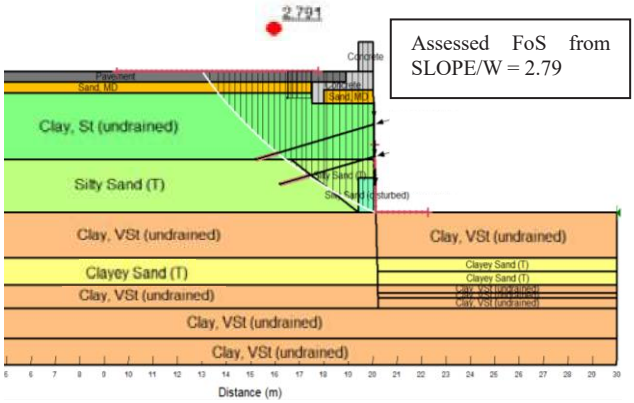

Figure 16. Assessed critical failure surface and FoS using limit equilibrium method

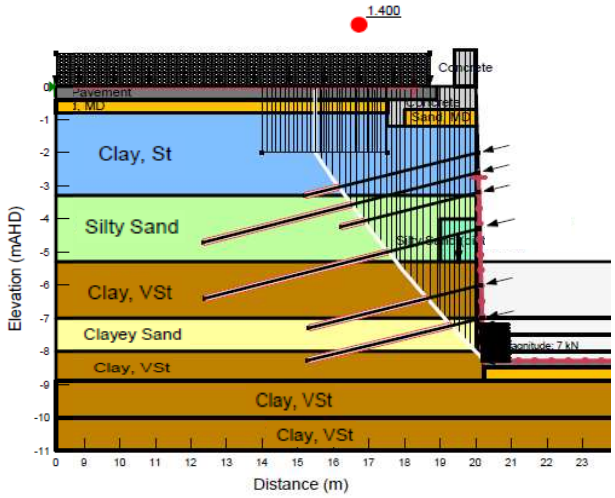

Figure 17. Remedial design with additional soil nails required to meet long term global stability requirements

## 8 CONCLUSIONS

The groundwater at the project site is below the design level of the lowered road. The non-fissured clay encountered over the excavation depth is unsaturated and stiff, with a lower bound soil suction value of pF = 3.6 considered for long-term wetted soil condition and pF = 3.4 for the adverse case of a prolonged leakage from a broken water pipe. The shear strength of the unsaturated clay, quantified by soil suction, was significantly greater than that derived based on conventional saturated soil mechanics. This allowed the use of a relatively light-weight retaining structure with considerable cost savings. The adopted retention system for the excavation is soil nail with a typically 75mm thick fiber shotcrete facing. For an 8 m high wall excavation in unsaturated clay, three rows of 4.5 to 6m long soil nails are required. The vertical and horizontal spacing between nails are 2.5m and 3m, respectively.

The subject soil nail wall in the unsaturated clay was not immune to construction issues. The excavation through some of the thick and clean sand lenses within the clay profile caused significant over-break, leading to greater wall movements than anticipated. An observational approach was implemented to cope with the soil variability and to reduce the risks of over-break. This required the presence of geotechnical site representatives to inspect the exposed face and select a suitable soil nail arrangement from the design toolbox (predefined designs for a range of possible soil profiles). Other construction issues encountered include (1) the adverse impact of a redundant sewer trench on the wall excavation in proximity; (2) the lower-than-expected soil nail bond stresses indicated in some proof load test results; and (3) the difference in performance of conventional steel reinforcing bar and self-drilling nail with sacrificial drill bit.


Figure 18. Soil nail wall after full depth excavation

## 9 ACKNOWLEDGEMENTS

The authors acknowledge the work of many others, including Aurecon, the Department of Planning, Transport and Infrastructure (DPTI), CPB Contractors, York Civil, Mott MacDonald, WGA, and Mr Richard Herraman formerly of DPTI, that made the project a success.

## 10 REFERENCES

AS4678-2002 Earth Retaining Structures. Standards Australia.

Briaud J-L., (2013) Geotechnical engineering: Unsaturated and saturated soils. John Wiley & Sons.

CIRIA C760 - Gaba A.R., Hardy S., Doughty L., Powrie W. and Selemetas D. (2017). Guidance on embedded retaining wall design CIRIA Report C760, London: CIRIA.

Desa, S.A.J., Scott, B.T. (2018). Inferring soil water characteristics for Adelaide clay using fractal theory. Australian Geomechanics J., Vol. 53, No.1, pp.127 – 135.

Fredlund, D. G., Rahardjo, H. (1993). Soil Mechanics for Unsaturated Soils. John Wiley & Sons.

Kaggwa, W.S. (1992), On in situ stresses, soil suction, undrained shear strength and $K_0$ of expansive clays from Adelaide City, Civil Eng. Trans., IEAust, Vol. CE34, Vol.2, pp. 97-106.

Khalili, N., Khabbaz, M.H. (1998). A unique relationship for $\chi$ for the determination of the shear strength of unsaturated soils. Géotechnique. 39(5): 681-687.

Richards, B.G. (1977), Pressures on a Retaining Wall by an Expansive Clay. Proc. 9th ICSMFE, 2/72, pp. 705-710, Tokyo.

Woodburn, J. A. (1997) Report No GSU 1061 for the Department of Planning, Transport and Infrastructure of SA.